Chapter

6

Catharanthus roseus cell suspensions overexpressing geraniol synthase in the plastid and cytosol

Mohd Zuwairi Saiman[1,2], Karel Miettinen[3], Natali Rianika Mustafa[1,4], Young Hae Choi[1], Robert Verpoorte[1], Anna Elisabeth Schulte[1,4]

[1]Natural Products Laboratory, Institute of Biology, Leiden University, 2300 RA Leiden, The Netherlands

[2]Institute of Biological Sciences, Faculty of Science, University of Malaya, 50603 Kuala Lumpur, Malaysia

[3]Plant Cell Physiology, Institute of Biology, Leiden University, 2300 RA Leiden, The Netherlands

[3]ExPlant Technologies B.V., Galileiweg 8 2333 BD Leiden, The Netherlands

Abstract

Previous studies showed that geraniol, an upstream precursor in the monoterpenoid pathway, could be a limiting factor for terpenoid indole alkaloid (TIA) production in *Catharanthus roseus* cells and hairy root cultures. This shortage in precursor availability could be due to limited expression of the geraniol synthase gene, and consequently a low activity of the encoded enzyme, which is located in the plastid and catalyzes the conversion of geranyl diphosphate to geraniol, or to the limitation of geraniol transport from the plastid to the cytosol. In the present study, *C. roseus* geraniol synthase was overexpressed in the plastid (CrGES) and cytosol (ΔplCrGES) of a non-TIA producing *C. roseus* cell culture via biolistic transformation. Transient expression studies confirmed the localization of the enzyme in the targeted subcellular compartments. Expression of the geraniol synthase was verified by Northern blot and reverse transcription-PCR. Neither TIA nor iridoid precursors were detected by HPLC-DAD in the transformed *C. roseus* cell cultures. Nevertheless, metabolomics analysis by NMR shows that the levels of phenylalanine, tyrosine, valine, and leucine were significantly higher in the CrGES overexpressing lines, while being lower in the ΔplCrGES overexpressing lines, compared to the controls. Isoleucine and tryptophan levels were also higher in the CrGES than the ΔplCrGES overexpressing lines. Apparently, overexpression of CrGES in the plastids and ΔplCrGES in the cytosol caused different effects on several primary metabolites including some derived from the shikimate pathway.

Introduction

Catharanthus roseus (Madagascar periwinkle) is a medicinal plant which produces a class of secondary metabolites called terpenoid indole alkaloid (TIA). More than 130 TIAs have been isolated from *C. roseus* and some of them are important pharmaceuticals such as the antihypertensive drugs ajmalicine and serpentine, and the antineoplastic agents vinblastine and vincristine (van der Heijden et al. 2004). However, most TIAs are produced at low levels in the plant, particularly the valuable chemotherapy drugs vinblastine and vincristine which are present only in trace amounts, resulting in high market price.

Biotechnological approaches using *in vitro* cell and tissue cultures of *C. roseus* have been developed as an alternative source of TIA. However, a high producing cell line has not been obtained despite all efforts in the optimization of growing and production conditions (Moreno et al. 1995). Although the mass cultivation of *C. roseus* cells is feasible in a large-scale bioreactor, the cost of production of alkaloids is too high for commercialization

(Verpoorte et al. 2000). Metabolic engineering by overexpressing the biosynthetic genes of the target pathway or suppressing flux of competing pathways are promising approaches to improve the production of TIA in *C. roseus* cell cultures (Verpoorte et al. 2000; Verpoorte et al. 2002; Zhao and Verpoorte 2007). Single or multiple genes encoding the biosynthesis enzymes of the TIA pathway have successfully been overexpressed (anthranilate synthase: AS, 1-deoxy-D-xylulose synthase: DXS, tryptophan decarboxylase: TDC, strictosidine synthase: STR, geraniol 8-oxidase: G8O (also known as geraniol 10-hydroxylase: G10H), desacetoxyvindoline 4-hydroxylase: DAT, apoplastic peroxidase: CrPrx) in *C. roseus* cells (Canel et al. 1998), hairy roots (Magnota et al. 2007; Peebles et al. 2010; Wang et al. 2010; Jaggi et al. 2011), and plants (Pan et al. 2012). In addition, overexpression of the transcription factors ORCA2 (Liu et al. 2011) and ORCA3 (van der Fits and Memelink 2000; Peebles et al. 2009; Wang et al. 2010; Pan et al. 2012), and an ATP-binding cassette (ABC) transporter (Pomahačová et al. 2009) were studied in *C. roseus,* which resulted in elevated level of some TIAs. However, the precursors from primary metabolism seem to be the limiting factor in increasing production. Channeling of the metabolic flux towards TIA biosynthesis seems thus on important target for metabolic engineering to improve TIA production and to reduce the production costs with plants or plant cell cultures.

Metabolic engineering requires knowledge on the biosynthesis pathway of the products of interest, the subcellular compartmentation of specific steps in the pathway, and the transport of the intermediates between intracellular compartments and between different cell types. The biosynthesis of TIA in *C. roseus* is a complex metabolic pathway requiring precursors from two different biosynthetic routes, i.e. tryptamine from the shikimate/tryptophan pathway and secologanin from the iridoid pathway. Condensation of tryptamine and secologanin produces strictosidine, the central intermediate of TIAs. Among the two precursor pathways, the iridoid pathway is considered a major rate-limiting factor for TIA production in *C. roseus* cell cultures (Whitmer et al. 2002; van der Heijden et al. 2004; Zhao and Verpoorte 2007).

The iridoid precursors of the TIA derive from 8-hydroxygeraniol (also known as 10-hydroxygeraniol) which is formed upon hydroxylation of geraniol generated from geranyl diphosphate (GPP). Geranyl diphosphate is a condensation product of the basic isoprene units, isopentenyl diphosphate (IPP) and dimethylallyl diphosphate (DMAPP). In plants, IPP and DMAPP are produced via two different metabolic pathways each leading to a distinct set of terpenoid derivatives. These two pathways closely interact but they are separated on

subcellular level, i.e. the cytosolic/peroxisomal mevalonate pathway (MVA) and the plastidial methyl-erythritol phosphate (MEP) pathway (Rohmer 1999; Sapir-Mir et al. 2008; Simkin et al. 2011; Pulido et al. 2012). The iridoid/terpenoid moiety of TIA derives from GPP produced via the MEP pathway (Contin et al. 1998). This intermediate is primarily produced by the plastidial enzyme geranyl diphosphate synthase (GPPS), but can also be released as an intermediate during the formation of farnesyl diphosphate (FPP) catalyzed by FPP synthase (FPPS), which is localized in the peroxisome/cytosol (Martin et al. 2007; Thabet et al. 2011). Although the GPP production in the mevalonate pathway remains unclear, a few studies indicate that a low GPP pool was available in the cytosol for the synthesis of limonene in transgenic *Nicotiana tabacum* (Wu et al. 2006) and geraniol in transgenic *N. benthamiana* (Dong et al. 2013).

Several key biosynthesis enzymes in the TIA pathway have been characterized and overexpressed in *C. roseus.* Recently, the enzyme that catalyzes the conversion of GPP into geraniol, i.e. geraniol synthase (CrGES) has been isolated and characterized from *C. roseus* (Simkin et al. 2013). This enzyme is of interest since geraniol is considered as the limiting upstream precursor in TIA biosynthesis; feeding geraniol increased tabersonine and ajmalicine production in *C. roseus* hairy roots (Morgan and Shanks 2000) and cell suspension cultures (Lee-Parsons and Royce 2006), respectively. In the present study, we overexpressed CrGES, a plastidial localized-enzyme, in *C. roseus* cell cultures via biolistic transformation to increase the overall availability of geraniol for TIA biosynthesis. To evaluate and overcome a possible limitation in transport of geraniol from the plastid to the cytosol or other limitations in the plastidial MEP pathway, ΔplCrGES was expressed in the cytosol by removing the plastidial leader peptide in CrGES. It is conceivable that through ΔplCrGES expression in the cytosol, the mevalonate pathway can be directly linked to the TIA pathway and thus possibly lead to increased TIA biosynthesis by feeding mevalonic acid. In this study, changes in the levels of TIAs, precursors, and metabolites in the transformed *C. roseus* cells were determined.

Materials and methods

Cell culture

Catharanthus roseus cell suspension cultures (cell-line MP183L) were subcultured weekly by transferring 10 ml culture into 50 ml of Linsmaier and Skoog (LS) medium (Linsmaier and Skoog 1965) containing 30 g/l sucrose, 2 mg/l NAA, and 0.2 mg/l kinetin.

The cultures were grown on a gyratory shaker at 120 rpm at 25 ^{o}C in 16/8 hour light/dark regime (20 µE/m^2/sec) at 70% relative humidity.

Cloning, vector constructions and transformation

A full fragment of *C. roseu*s geraniol synthase (CrGES, Genbank ID: JN882024, Simkin et al. 2013, **Supplement 1**) or a truncated version of CrGES lacking the plastidial leader peptide (ΔplCrGES) were produced by a PCR-based strategy. For transient expression, constitutive, and inducible constructs; the forward primers for CrGES and ΔplCrGES were 5'GTCGACAAAATGGCAGCCACAATTAGTAACC-3' and 5'-GTCGACAAAATG TCTCTGCCTTTGGCAACT-3', respectively. The reverse primer for the transient expression study was 5'-GTCGACAAAACAAGGTGTAAAAAACAAAGC-3'; while for constitutive and inducible constructs, the reverse primer was 5'-TCTAGATTAAAAACAAGGTGTA AAAAACAAAGC-3' (**Supplement 2**). Fragments were amplified by PCR (MyCycler Thermal Cycler, Biorad) with following procedures: 98 °C, 1 min; 35 cycles, 98 °C, 15 sec; 57 °C, 20 sec; 72 °C, 1 min; 72 °C, 5 min. The PCR products were first cloned into a pJET1.2/blunt cloning vector (Thermo Scientific, Pittsburgh, PA, USA) and sequenced for confirmation. Subsequently, the verified CrGES and ΔplCrGES fragments were ligated into 1) pTH2-Δ*EcoRI* plasmid excised with *SalI* (transient expression construct, Niwa 2003); 2) pRT101 plasmid excised with *XhoI/XbaI* (constitutive construct, Töpfer et al. 1987); 3) pER8 plasmid excised with *XhoI/SpeI* (inducible construct, Zuo et al. 2000) (**Fig. 1A – C**).

Plasmids containing CrGES and ΔplCrGES were introduced into *C. roseus* cells via biolistic transformation (van der Fits and Memelink 1997). The control cells were transformed with the corresponding plasmid without insert. For transient expression and subcellular localization studies, transformed cells were placed on solid LS medium and viewed after 24 hours using a Zeiss Observer laser scanning microscope equipped with fluorescence filters. The transformed cells with constitutive or inducible expression constructs were cultured on solid LS medium containing 50 µg/ml hygromycin. The individual putative transgenic calli grown on this selective medium were converted to cell suspensions and subcultured every week by transferring 10 ml of cell suspension into 50 ml LS medium containing 30 g/l sucrose, 2 mg/l NAA, 0.2 mg/l kinetin, and 50 mg/l hygromycin.

Estradiol treatment and cell harvesting

At the fifth day after subculturing, the inducer *β*-estradiol (Sigma) dissolved in DMSO was added at a concentration of 10 µM into 10 ml aliquots of the inducible transgene cell suspensions. Control cells were treated with DMSO at a final concentration of 0.1% (v/v). Estradiol-induced cells and controls were harvested 24 hours after the treatments. Unless mentioned otherwise, cells containing constitutive transgenes did not receive any treatment and the cell cultures were harvested one week after subculturing. Harvested cells were immediately frozen in liquid nitrogen. Aliquots of the samples were stored at -80 ^{o}C for RNA extraction and the remaining biomass was lyophilized for 72 hours prior to metabolite analysis.

RNA extraction, Northern blot, reverse transcriptase-PCR

Frozen cells were ground to a fine powder in liquid nitrogen. Total RNA was extracted with two volumes of hot phenol buffer (1:1 mixture of phenol and 100 mM LiCl, 10 mM Na-EDTA, 1% SDS, 100 mM Tris) and one volume of chloroform. RNA was precipitated overnight with LiCl at a final concentration of 2 M, washed twice with 70% ethanol, and suspended in water.

Northern blot analysis was performed as described by Memelink (1994) with some modifications. Ten µg RNA samples were subjected to electrophoresis on 1.5% agarose/1% formaldehyde gels, and blotted to GeneScreen nylon membranes (Perkin-Elmer Life Science, Boston, MA, USA). Blots were prehybridized for several hours in 1M NaCl, 10% dextran sulfate (sodium salt, Sigma), 1% SDS, and 50 µg/ml denatured salmon sperm DNA at 65 ^{o}C before addition of denaturated ^{32}P-labeled DNA probes. After overnight hybridization, blots were washed twice at 42 ^{o}C for 30 min with 0.1 x SSPE (saline/sodium/phosphate/EDTA) and 0.5% SDS. Finally, the blots were washed briefly with 0.1 x SSPE at room temperature. Blots were exposed to X-ray films (Fuji, Tokyo, Japan).

Reverse transcription was carried out using the Revert Aid^{TM} H Minus First Strand cDNA Synthesis Kit (Fermentas) following to the manufacturer's instruction. The cDNA synthesized from each sample was used as template in PCR. Negative controls were performed by excluding reverse transcriptase enzyme in the reaction.

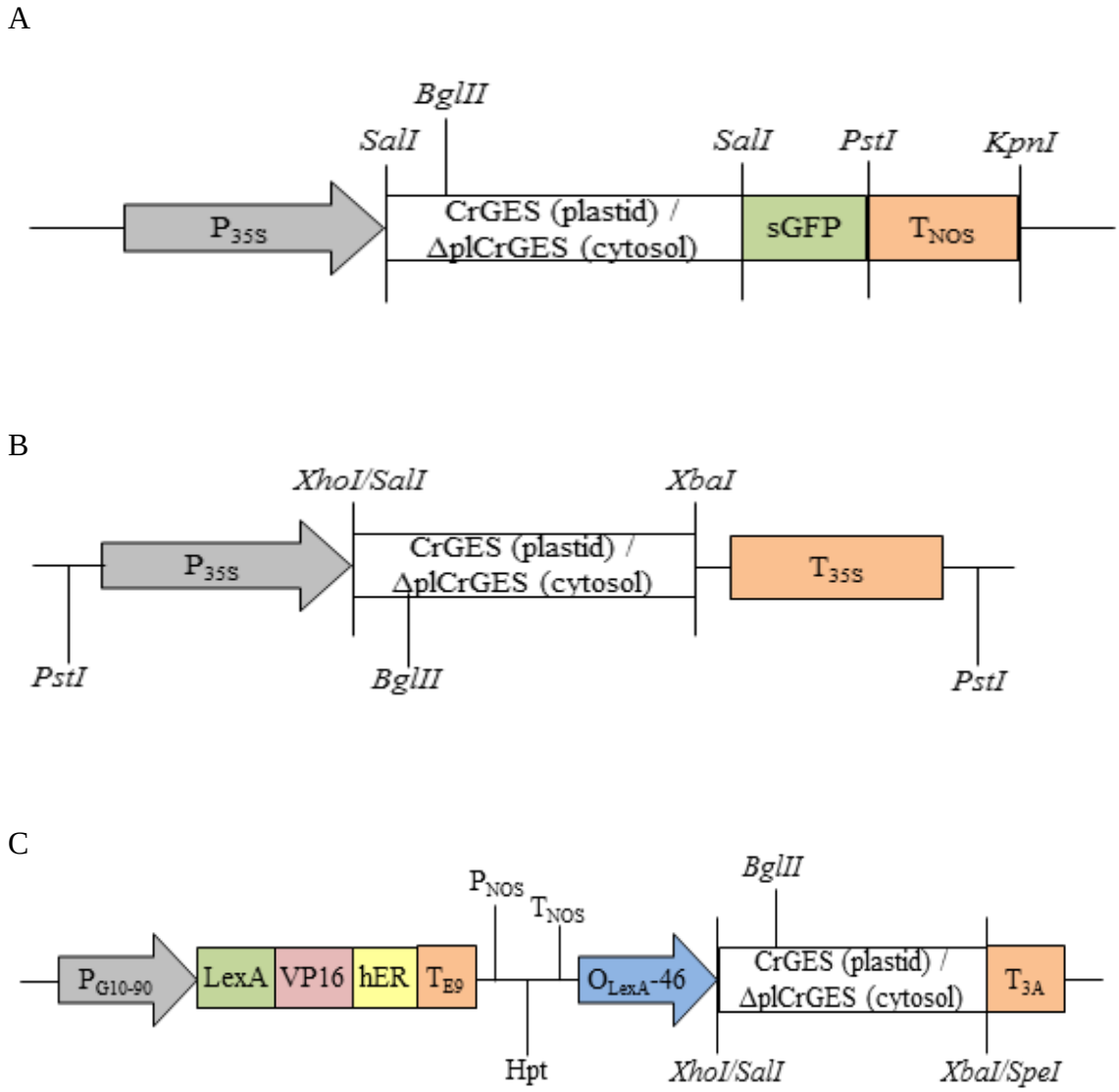

Fig. 1 Schematic representation of the constructs A) pTH2-Δ*EcoRI* (Niwa 2003); B) pRT101 (Töpfer et al. 1987); C) pER8 (Zuo et al. 2000) vectors containing either the full-length fragment of *Catharanthus roseus* geraniol synthase (CrGES) or the truncated CrGES without plastidial leader peptide (ΔplCrGES) that are targeting the enzyme to the plastid or the cytosol, respectively. P_{35S}: cauliflower mosaic virus 35S promoter, sGFP: synthetic green fluorescence protein (S65T), T_{NOS}: nopaline synthase terminator, T_{35S}: cauliflower mosaic virus 35S terminator, $P_{G10\text{-}90}$: a synthetic promoter controlling XVE (Ishige et al. 1999), LexA *E. coli* repressor DNA binding domain, VP16: herpes simplex viral protein 16, hER: hormone-binding domain of human estrogen receptor, T_{E9}: pea rbcS E9 terminator, P_{NOS}: nopaline synthase promoter, Hpt: hygromycin phosphotranferase II coding sequence, O_{LexA}: operator region of LexA promoter, -46: TATA box of 35S promoter, T_{3A}: pea rbcS 3A terminator.

Jasmonic acid elicitation

Jasmonic acid (Sigma) at a final concentration of 100 µM was fed to the cell suspensions containing the constitutive transgenes at the fifth day after subculturing. Subsequently, the treated cultures were harvested at 24, 48, and 72 hours after elicitation. Samples were freeze-dried for 72 hours and stored for TIA analysis.

Analysis of terpenoid indole alkaloids

Freeze-dried cells (100 mg) were extracted with 5 ml methanol, vortexed, sonicated for 20 min, and centrifuged for 30 min (3,500 rpm). The dried supernatant was suspended in 1 ml phosphoric acid (1 M). Samples were subjected for terpenoid indole alkaloid and precursor analysis using high performance liquid chromatography-diode array detector (HPLC-DAD) (Agilent Techologies Inc., Santa Clara, CA, USA) as described by Saiman et al. (2014).

Geraniol analysis

Freeze-dried cells (100 mg) were extracted with 5 ml dichloromethane, vortexed, ultrasonicated 10 min, and centrifuged for 10 min (3,000 rpm, 4 ^{o}C). The eluent was concentrated under a flow of nitrogen and 1 µl of concentrated extract was injected into gas chromatography-mass spectroscopy (GS-MS) (Agilent Technologies Inc.) equipped with a DB-5 capillary column (30 m x 0.25 mm i.d., film thickness of 0.25 um) (J&W Scientific Inc., Folsom, CA, USA). The initial oven temperature was 45 ^{o}C for 1 min, and was increased to 300 ^{o}C at a rate of 10 ^{o}C/min and held for 5 min at 300 ^{o}C. Geraniol standard compound (Sigma) was used for identification.

NMR and multivariate data analysis

Freeze-dried cells (25 mg) were extracted with 1:1 CD_3OD:KH_2PO_4 buffer in D_2O (pH 6.0, containing 0.01% trimethylsilyl propanoic acid [TMSP] as internal standard). The mixture was vortexed for 10 sec, sonicated for 10 min, and centrifuged for 15 min (14,000 rpm). Samples were analyzed using 500 MHz NMR (Bruker, Karlsruhe, Germany). NMR spectra were manually phased, baseline corrected, and calibrated to TMSP at 0.0 ppm using XWIN NMR version 3.5 (Bruker). AMIX software (Bruker) was used for bucketing (width δ 0.04) and data reduction of the ^{1}H-NMR spectra (δ 0.40 – 10.00) using total intensity scaling. Multivariate data analysis was performed with the SIMCA-P+ software version 12.0

(Umetrics, Umeå, Sweden). Analysis of variance (ANOVA) followed by Duncan's Multiple Range Test (DMRT) was performed on IBM SPSS Statistics 20 (SPSS Inc., Chicago, IL, USA) to determine statistical differences ($P < 0.05$) between means of groups.

Results and discussion

Cloning, vector constructs, and transformation

The geraniol synthase gene of *C. roseu*s (CrGES) was recently characterized by Simkin et al. (2013). It has a 1770 bp DNA sequence and encodes a protein of 589 amino acids in length. CrGES is localized in plastids as suggested by the leader peptide encoded in its cDNA (Simkin et al. 2013). To overexpress CrGES in the plastid and in the cytosol, a full-length CrGES fragment and a truncated version of CrGES lacking the first 156 coding nucleotides (ΔplCrGES) were constructed. Primers were designed for three different vectors employed for different purposes, i.e. pTH2-Δ*EcoRI* for transient expression and subcellular localization studies, pRT101 for constitutive expression, and pER8 for estradiol-inducible transgene expression. The pTH2-Δ*EcoRI* plasmid used in this study is a derivative of pTH2 by adding the "EKE" linker in the *EcoRI* site resulting in loss of the *EcoRI* site and introduction of a *KpnI* site. The pTH2 plasmid has been widely used to study subcellular localization because it encodes the synthetic green fluorescent protein (sGFP: S65T, Niwa 2003). To insert CrGES or ΔplCrGES fragments between the CaMV 35S promoter and sGFP in the pTH2-Δ*EcoRI*, a *SalI* site was introduced at the 5' and 3' of the inserts. For constitutive and inducible expression constructs, CrGES and ΔplCrGES fragments were amplified with a *SalI* site at the 5' and *XbaI* site at the 3', which is compatible with *XhoI/XbaI* and *XhoI/SpeI* sites in the pRT101 and pER8 plasmid, respectively. The PCR products were excised with restriction enzymes and examined in gel electrophoresis (**Supplement 3**). Subsequently, the PCR products were cloned in the pJET1.2/blunt cloning vector (Thermo Scientific). This vector is much easier for cloning and has high positive clone efficiency. In addition, the insert fragment cloned in this vector can be directly checked by sequencing. After DNA sequencing and verifying the correct sequence, the CrGES and ΔplCrGES fragments were ligated into the pTH2-Δ*EcoRI*, pRT101, and pER8 plasmids and subsequently multiplied in *E. coli*. The constructs were examined with restriction enzymes after the plasmids were purified from *E. coli* (**Supplement 4 – 6**).

Transformation of the vectors containing CrGES or ΔplCrGES into *C. roseus* cells was realized via particle bombardment. Initially, two wild-type lines of *C. roseus* cell

suspensions were used for transformation, i.e. the MP183L and the CRPP line. Both cell lines are different in phenotype and metabolites. CRPP is a high producing-TIA cell line, which accumulates among others the secoiridoid precursor loganic acid, and the alkaloids strictosidine, serpentine, tabersonine, and catharanthine. On the other hand, the MP183L line accumulates only the TIA precursors tryptophan and tryptamine, but no secoiridoid precursors nor TIA under the standard growth conditions. Nevertheless, the MP183L line is commonly used for transformation studies in our laboratory as it is easily transformed and giving stable transgenic cell lines. **Figure 2** shows the putative transformed MP183L calli carrying the antibiotic selectable marker, grown on LS medium supplemented with hygromycin. The average numbers of transformed MP183L calli grown per plate were 10 and 26 for pRT101 and pER8 construct, respectively. However, the bombarded CRPP cells did not produce any callus on the selection medium due to unsuccessful transformation. As compared to the fine cells of MP183L, the CRPP cells form aggregates which may affect the transformation efficiency. An additional transient expression study using the GUS assay for evaluation also showed a better transformation efficiency in MP183L compared to the CRPP cell line (**Supplement 7**).

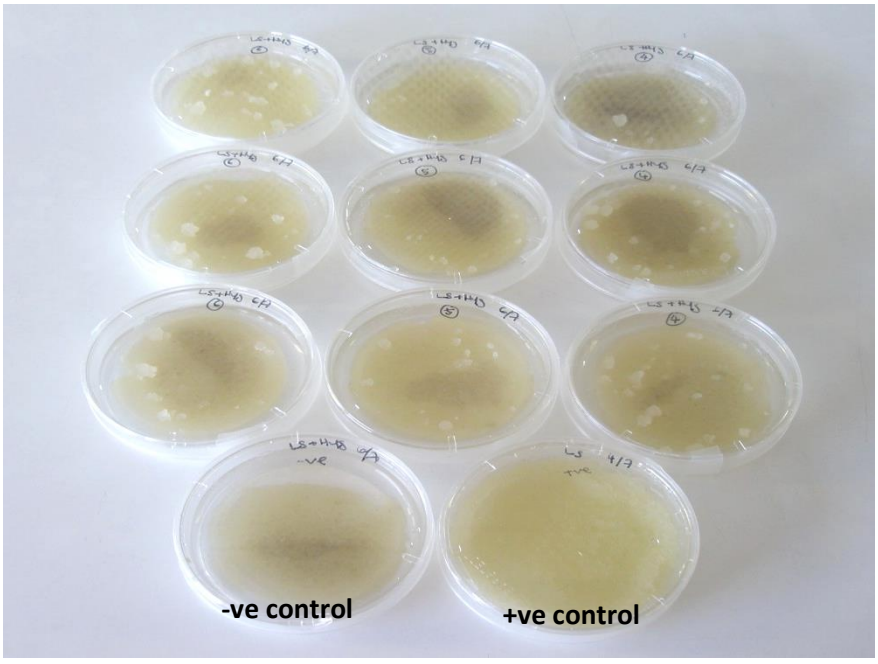

Fig. 2 *Catharanthus roseus* cells bombarded with inducible constructs of CrGES and ΔplCrGES generate putative transformed calli on the culture medium containing hygromycin as selection marker.

Subcellular localization study

To confirm the subcellular localization of CrGES and ΔplCrGES, the transient expression of the construct pTH2-Δ*EcoRI*::CrGES-GFP and pTH2-Δ*EcoRI*::ΔplCrGES-GFP was analyzed in the transformed *C. roseus* cells (MP183L line). The results show that the truncated CrGES without plastidial leader peptide fused with GFP (ΔplCrGES-GFP) was displaying fluorescence in the cytosol (**Fig. 3A – B**). In accordance to Simkin et al. (2013), the full length CrGES-GFP fusion protein signal was located in the plastid stroma and stromules (**Fig. 3C**). To further confirm the subcellular compartments, we co-bombarded the CrGES-GFP and plastid-mCherry marker (Nelson et al. 2007) in the *C. roseus* cells. The results show that the fluorescence signal of CrGES-GFP matched with those of the plastidial marker (**Fig. 3D**), thus confirming its localization in the plastid stroma and stromules. After removing its plastidial leader peptide, the enzyme was expressed in the cytosol.

Gene expression

Expression of CrGES and ΔplCrGES in the putatively transformed *C. roseus* cells was analyzed using Northern blots. **Figure 4A and 5A** show the expression of CrGES and ΔplCrGES in some lines of the *C. roseus* cells transformed with the constitutive or the estradiol-inducible construct, respectively. However, the Northern blot analyses displayed some background noise and tailing possibly caused by the probe or membrane. To verify the results of the Northern blot analyses, reverse transcriptase PCR (RT-PCR) was performed on the same purified RNA. The RT-PCR results reveal the expected sizes of the CrGES and ΔplCrGES fragments with a relatively similar expression level as shown in the Northern Blot (**Fig. 4A – B and 5A – B**). Therefore, these results confirm the overexpression of the CrGES (plastid) and ΔplCrGES (cytosol) in both constitutive and estradiol-induced transgenic *C. roseus* cell suspensions.

Terpenoid indole alkaloid analysis

It was of interest to analyze TIA production in the *C. roseus* cells overexpressing geraniol synthase, particularly to compare the difference between plastidial and cytosolic CrGES overexpression lines. Therefore, several lines of constitutive and inducible transgene *C. roseus* cells were selected and analyzed for the TIA, iridoid and indole precursors using an HPLC-DAD platform.

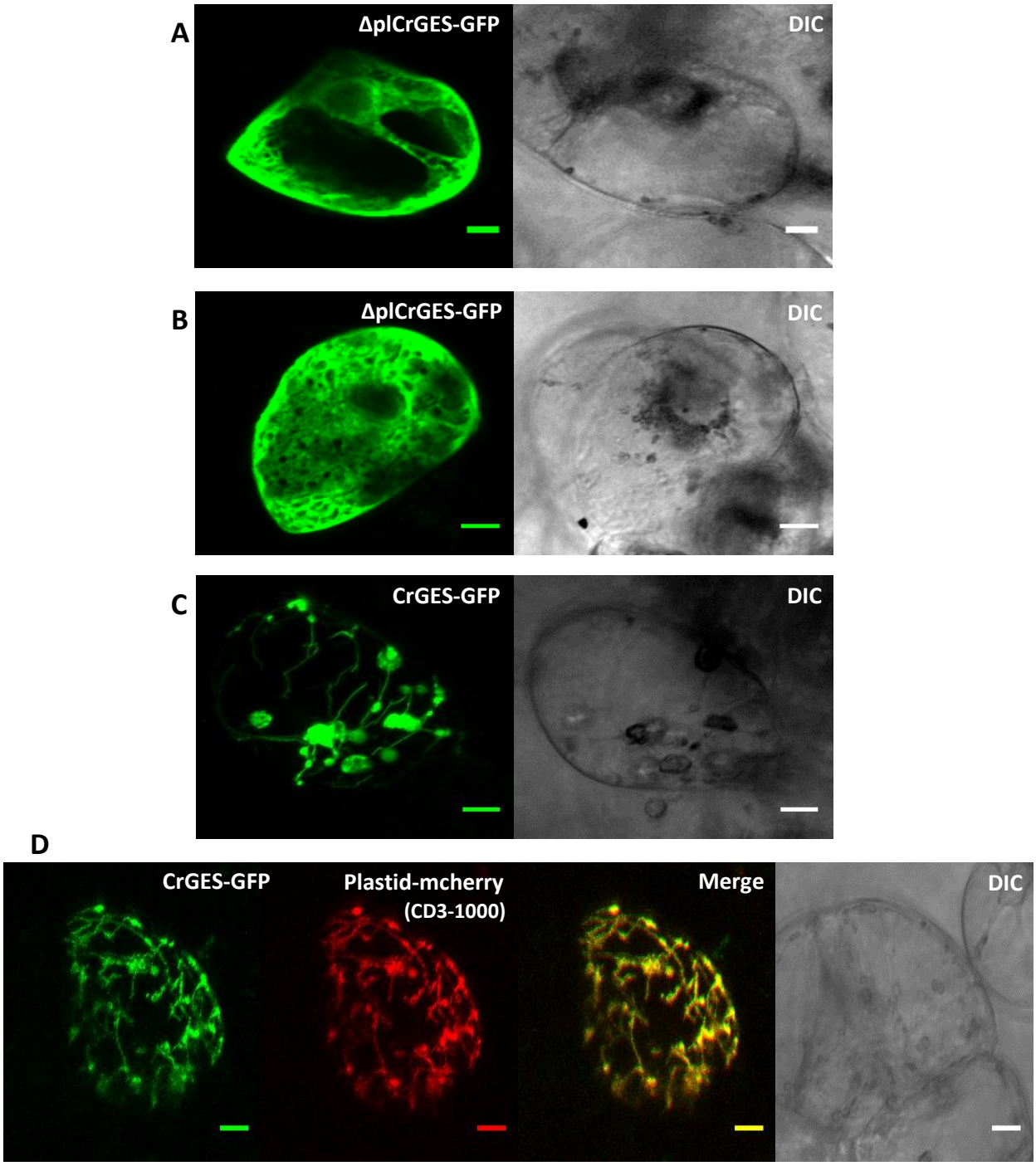

Fig. 3 Subcellular localization of ΔplCrGES-GFP (A, B) and CrGES-GFP (C) in cytosol and plastid/stromules of *Catharanthus roseus* cells, respectively. Co-localization of the two fluorescence signals appeared in yellow when merging the two individual (green/red) color images (D). The cell morphology is observed with differential interference contrast (DIC) microscopy. Bars correspond to 10 µm.

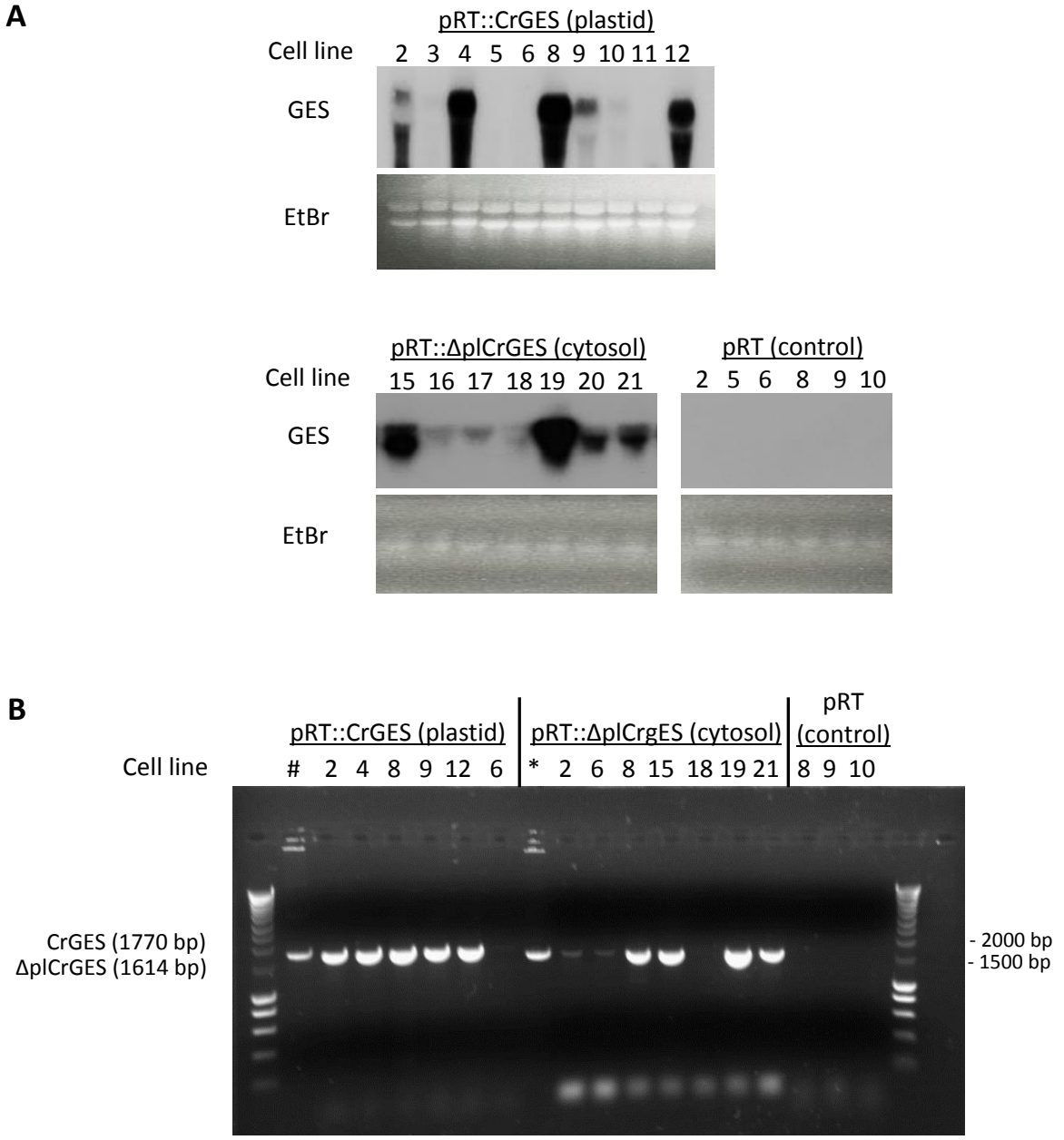

Fig. 4 Northern blot (A) and RT-PCR (B) analysis of independent transgenic *Catharanthus roseus* cell lines constitutively overexpressing CrGES (plastid), and ΔplCrGES (cytosol) versus cells transformed with the corresponding empty vector (control). Analysis of gene expression using Northern blot shows noise and tailing signals and therefore RT-PCR is used to supplement expression data. The ethidium bromide stained gel (EtBr) is shown as a control for RNA loading. # and * in RT-PCR represent the CrGES and ΔplCrGES fragments, respectively, which are used for comparing the sizes of the bands.

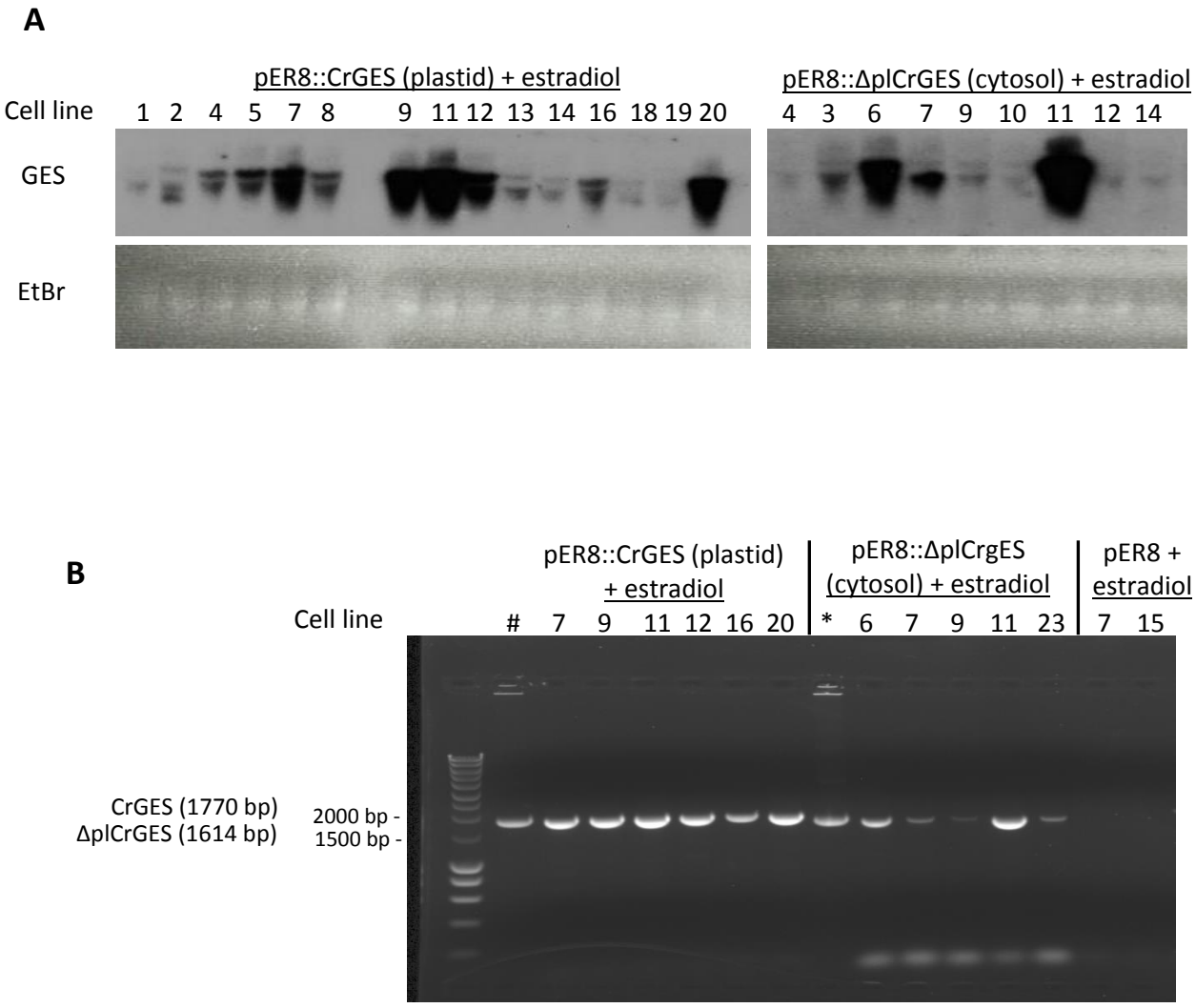

Fig. 5 Northern blot (A) and RT-PCR (B) analysis of independent transgenic *Catharanthus roseus* cell lines overexpressing estradiol-inducible CrGES (plastid), and ΔplCrGES (cytosol) versus control cells transformed with the corresponding empty vector. All samples were fed with estradiol (10 μM) at the fifth day after subculturing and harvested after 24 hours. Analysis of gene expression using Northern blot shows noise and tailing signals and therefore RT-PCR is used to supplement expression data. The ethidium bromide stained gel (EtBr) is shown as a control for RNA loading. # and * in RT-PCR represent CrGES and ΔplCrGES fragments, respectively, which are used for comparing the sizes of the bands.

Terpenoid indole alkaloids or iridoid precursors were not detected in any of these transformed *C. roseus* cell cultures, neither in constitutive nor inducible lines. Similar to the previous analysis of the wild-type *C. roseus* cell-line MP183L, only tryptophan and tryptamine were detected in the cultures. This indicates that geraniol synthase overexpression in the plastid or cytosol of these *C. roseus* cells does not directly enhance fluxes towards iridoid and TIA biosynthesis. Furthermore, in order to build a metabolic bridge between GPP from mevalonate pathway to the iridoids and subsequently induce TIA production, the upstream precursor mevalonic acid (0.5 µM final concentration) was fed to the transgenic *C. roseus* cells constitutively overexpressing ΔplCrGES. However, this did not induce any difference in production levels. A lack of one or more biosynthesis enzymes before or after geraniol synthase could be the reason that the transformed MP183L cell lines did not produce TIA or iridoid precursors. Our previous study showed that the CATL cell line; which derived from MPL183L line, has low gene transcript levels of DXR and G8O (also known as G10H) if compared to the TIA-accumulating CRPP cell line (Saiman et al. 2014). Overexpression of G8O (G10H) in *C. roseus* hairy roots (Wang et al. 2010) and plants (Pan et al. 2012) has increased the levels of several TIAs which indicates that the G8O (G10H) availability is critical for TIA production. It is thus of interest to overexpress CrGES in iridoid- or TIA-accumulating *C. roseus* cell cultures to study the carbon flux in the iridoid or TIA pathway.

The transgenic *C. roseus* cell lines in this study did not accumulate TIA or iridoid precursors, however other metabolic changes may have occurred in the transgenic cells, which is studied by NMR (see below). Nevertheless, to evaluate TIA production in the transformed MP183L line, the transgenic cell lines constitutively overexpressing CrGES or ΔplCrGES, and the control lines containing the empty vector were elicited with jasmonic acid (100 µM). Jasmonate is a defense signaling compound and is often used as elicitor to induce secondary metabolism in plant. Jasmonate elicitation has been reported to induce all known TIA pathway genes including *GES* (Simkin et al. 2013), *G8O* or *G10H* (Collu et al. 2001), *ASα, DXS, TDC, STR,* and *SGD* (van der Fits and Memelink 2000), resulting in increased levels of TIA in *C. roseus* cell suspension (El-Sayed and Verpoorte 2004; Vázquez-Flota et al. 2009). After elicitation, ajmalicine, tabersonine, and a tabersonine-like compound were detected in the cell cultures. Tryptamine levels increased after elicitation as jasmonic acid induces the expression of *TDC*, but no iridoid precursors were detected in the samples. **Figure 6** shows that most of the cell lines accumulated the alkaloids at 48 and 72 hours after

elicitation. The cell line ΔplCrGES #19 accumulated higher levels of alkaloids compared to the other cell lines. However, the alkaloid production levels in the control lines were quite variable upon elicitation; whereas one empty vector control line did not accumulate alkaloids after elicitation, control line #8 produced alkaloids at a comparable level to that produced by the CrGES or ΔplCrGES lines. In this perspective only line ΔplCrGES #19 revealed higher TIA production than controls. Therefore, we conclude that jasmonic acid elicitation did not cause a clear difference in TIA level between the geraniol synthase overexpressing cells and the controls as the elicitation effect seems to vary too much among the individual cell lines.

Geraniol analysis

No geraniol peak was detected by GC in the plastidial CrGES or cytosolic ΔplCrGES overexpressing cells, which might be due to 1) the lack of carbon-five precursors because of limiting activity of upstream biosynthesis enzymes, 2) competing pathways acting on GPP, e.g. leading to FPP and sterols or to GGPP and carotenoids, or 3) the conversion of geraniol to glycosylated derivatives. Dong et al. (2013) reported that tobacco plants overexpressing geraniol synthase from *Valeriana officinalis* (VoGES) predominantly accumulated geraniol glycoside. Therefore, further work needs to be done to either analyze the glycosylated geraniol compounds in the transformed MP183L lines or treat the cells with glycosidase to release geraniol and geraniol related compounds.

Expression of VoGES to the cytosolic mevalonate compartment resulted in 30% lower geraniol glycoside than the plastidial targeted VoGES (Dong et al. 2013). This indicates a smaller pool of GPP in the mevalonate pathway compared to the MEP pathway. It may be interesting to overexpress both GPPS and GES in the mevalonate pathway of *C. roseus* as Wu et al. (2006) showed that the co-expression of limonene synthase (LS) and GPPS in the cytosolic mevalonate pathway increased production of limonene 6-fold compared to the single overexpression of LS. However, the targeted subcellular compartment for GPPS expression in the mevalonate pathway needs to be evaluated since the IPP isomerase (Sapir-Mir et al. 2008) and FPPS (Thabet et al. 2011), which were generally regarded as cytosolic enzymes, were recently reported to be localized in peroxisomes. Nevertheless, Thabet et al. (2011) did not exclude the possibility that a certain proportion of the FPPS is also localized in the cytosol. Furthermore, down-regulation of FPPS may be an interesting approach since a mutated FPPS yeast strain overexpressing *Ocimum basilicum* geraniol synthase (ObGES) accumulated geraniol produced from the available GPP pool (Fischer et al. 2011).

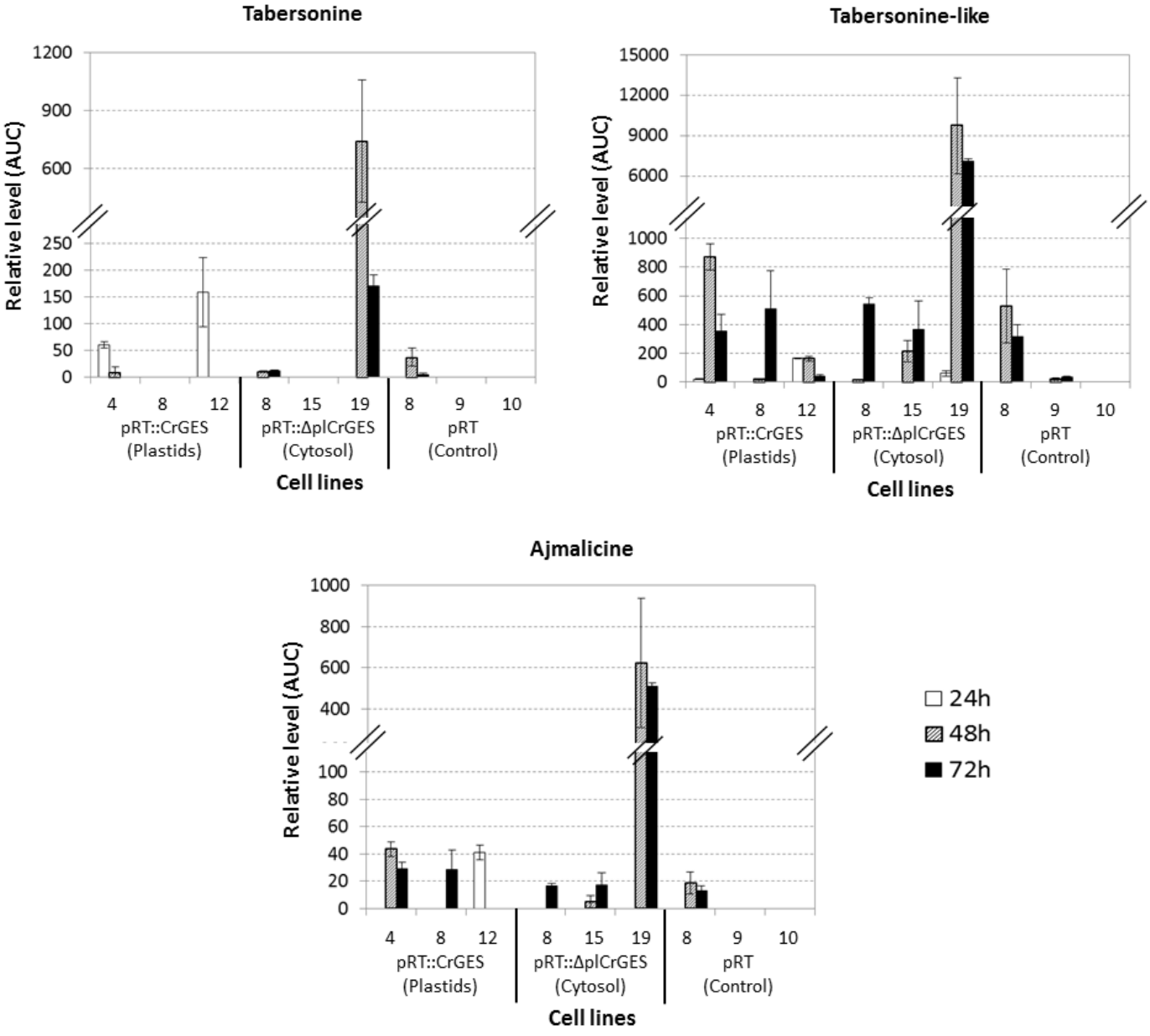

Fig. 6 Relative levels of terpenoid indole alkaloids (ajmalicine, tabersonine, and tabersonine-like compound) detected by HPLC-Diode Array Detector (DAD) in jasmonate-elicited *Catharanthus roseus* cell suspensions constitutively overexpressing CrGES (plastids; cell line 4, 8, and 12), ΔplCrGES (cytosol; cell line 8, 15, and 19) and empty vector pRT (control; cell line 8, 9, and 10). All samples were elicited with jasmonic acid (100 μM) at the fifth day after subculturing and harvested at 24, 48, and 72 hours after elicitation. Results are the mean of two replicates; error bars indicate the two values. AUC is area under the curve value.

NMR-based metabolomics and multivariate data analysis

In order to further investigate the metabolic differences in the non-elicited transformed *C. roseus* cells, NMR-based metabolomics was conducted and the ^{1}H-NMR data were subjected to multivariate data analysis. Principal component analysis (PCA) which is an unsupervised clustering method was initially performed to discriminate the samples. **Figure 7A** shows a PCA score plot of constitutive CrGES (three cell lines), ΔplCrGES (three cell lines), and control-empty vector (five cell lines). PC1 and PC2 explained 45% and 33% of variation, respectively. However, PCA did not clearly separate the different cell lines, which means that the variation between the groups is smaller than that within the individual cell lines. Therefore, partial least squares-discriminant analysis (PLS-DA) was applied to the same ^{1}H-NMR data to specifically examine the metabolite differences between the different construct lines.

Partial least squares-discriminant analysis (PLS-DA) is a supervised multivariate data analysis that uses information in another matrix. In addition to the X-matrix of NMR data, three groups (CrGES, ΔplCrGES, and empty vector) were assigned for the Y-matrix in PLS-DA. **Figure 7B** shows the PLS-DA score plot of the samples, in which the separation between the groups has considerably improved. The PLS-DA model was validated by the permutation method through 20 applications, in which the Q2 values of permuted Y vectors to the left were lower than the original ones to the right and the regression of Q2 lines intersect vertical axis at below zero (**Fig. 7C**). To get a better sample separation from the validated PLS-DA model, orthogonal projection to latent structures-discriminant analysis (OPLS-DA) was applied to the same data.

In OPLS-DA, a single component is used as a predictor for the class/group, while the other components describe the variation orthogonal to the first predictive component (Westerhuis et al. 2010). **Figure 7D** shows a clear separation between three groups (CrGES, ΔplCrGES, and empty vector) in the OPLS-DA score plot. All CrGES overexpressing cell lines were grouped in the positive area of component 1 and the negative area of component 2, while ΔplCrGES overexpressing cell lines were in negative areas of component 1 and 2, and the control cell lines (empty vector) were grouped in negative and positive area of component 1 and 2, respectively.

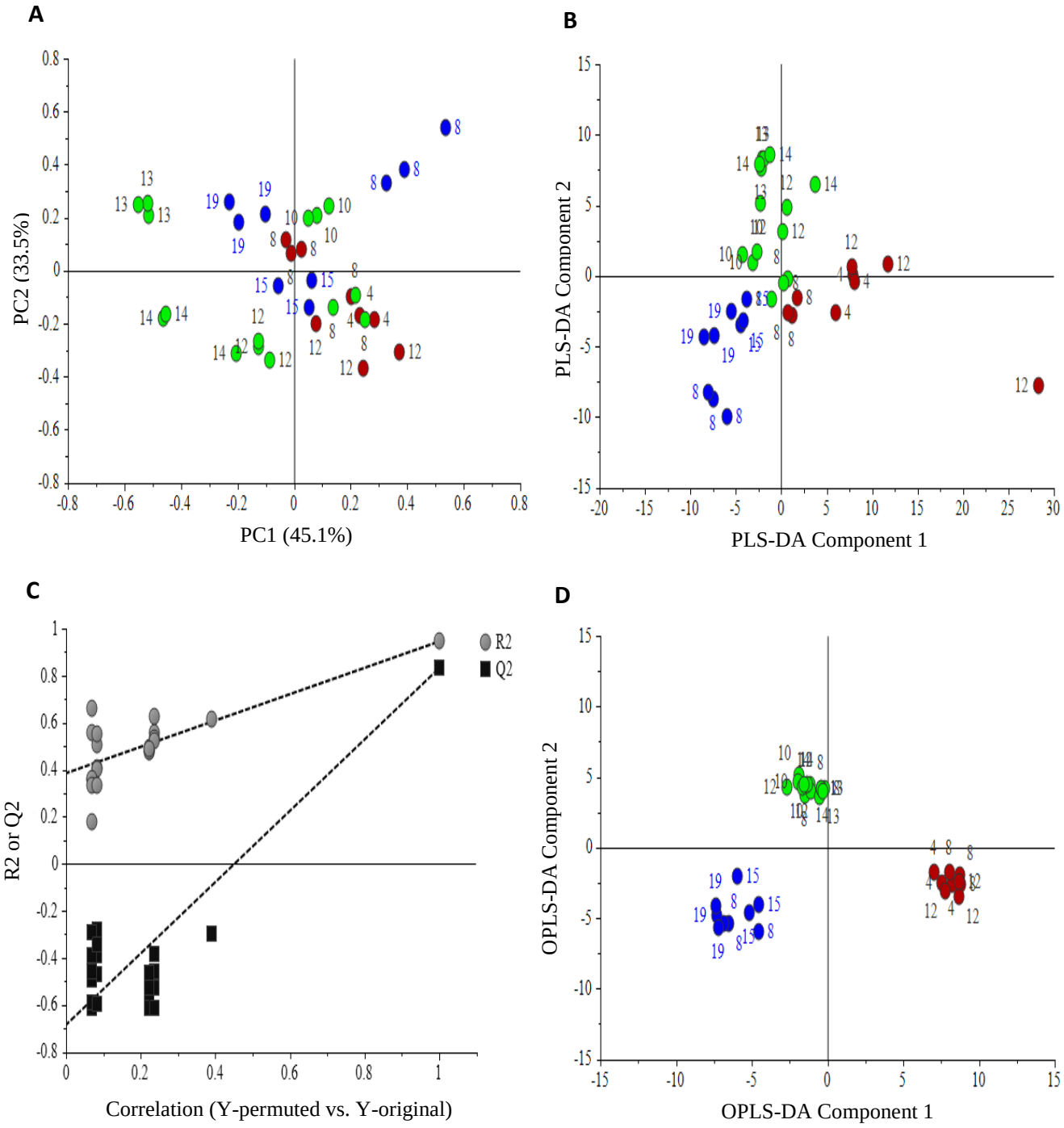

Fig. 7 Multivariate data analyses of *Catharanthus roseus* cells constitutively overexpressing CrGES (red color), ΔplCrGES (blue color), and the control *C. roseus* cells transformed with empty vector (green color). Principal component analysis (PCA) score plot (A), partial least squares-discriminant analysis (PLS-DA) score plot (B), and orthogonal projection to latent structures-discriminant analysis (OPLS-DA) score plot (D). The numbers in the score plots represent the cell-line label. Validation of PLS-DA by permutation test (C). R2 is a measurement of the model's goodness of fit. Q2 is a measurement of the predictive ability of the model.

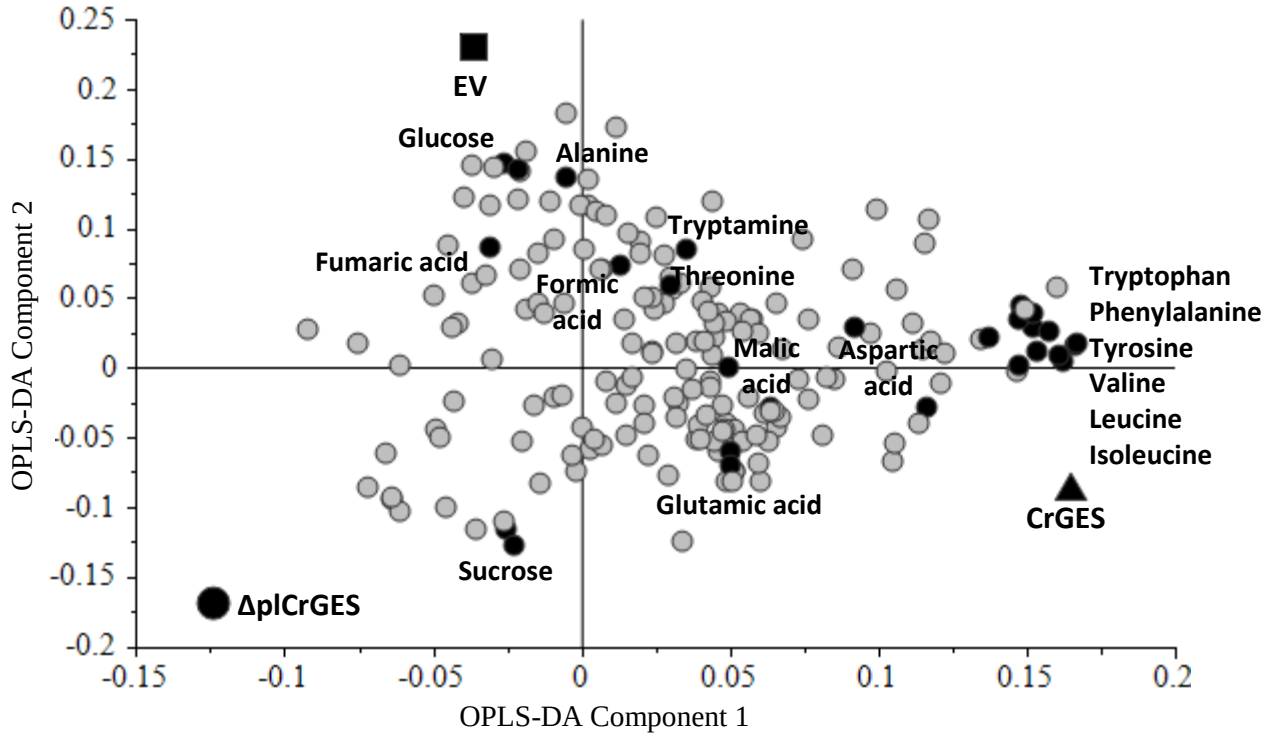

Fig. 8 Loading plot of orthogonal projection to latent structures-discriminant analysis (OPLS-DA) of *Catharanthus roseus* cells constitutively overexpressing CrGES, ΔplCrGES, and the control *C. roseus* cells transformed with empty vector (EV). Variables X (metabolite signals) located closely to variable Y (CrGES, ΔplCrGES, EV) contributes to the separation of the samples.

The NMR signals of some metabolites detected in the samples were assigned (**Table 1)**. The loading plot (**Fig. 8**) reveals which metabolites contribute to the separation of the groups. The result suggests that tryptophan, phenylalanine, tyrosine, valine, leucine, isoleucine, aspartic acid, malic acid, and glutamic acid are the metabolites that strongly influence the separation of the constitutive CrGES overexpressing cell lines. In the constitutive ΔplCrGES overexpressing cell lines, sucrose was associated to the separation of this group. Glucose, alanine, fumaric acid, and formic acid were detected close to the component area where the control lines were located, suggesting the influence of these metabolites for defining the control cell lines. **Figure 9** compares aromatic region of ^{1}H-NMR spectra of the different cell lines in the constitutive CrGES, ΔplCrGES, and the empty vector transformed *C. roseus* cell cultures.

In order to confirm that the metabolites are statistically significant for the separation of the groups, an ANOVA test ($P < 0.05$) was performed by comparing the mean value of the metabolites between the groups of observation; each group consists of three to five different

Table 1. ^{1}H chemical shift (δ in ppm) and coupling constants (J in Hz) of some metabolites detected in the transgenic and control cell cultures of *Catharanthus roseus. s* = singlet, *d* = doublet, *dd* = double doublet, *t* = triplet, *m* = multiplet

Compounds	**Chemical shift (ppm) and coupling constant (Hz)**
Leucine	δ 0.97 (*d*, J = 6.8); δ 0.99 (*d*, J = 6.8)
Isoleucine	δ 0.96 (*t*, J = 7.5); δ 1.03 (*d*, J = 7.0)
Valine	δ 1.01 (*d*, J = 7.0); δ 1.06 (*d*, J = 7.0)
Threonine	δ 1.34 (*d*, J = 6.6)
Alanine	δ 1.49 (*d*, J = 7.2)
Glutamic acid	δ 2.04 (*m*); δ 2.12 (*m*); δ 2.39 (*m*)
Glutamine	δ 2.13 (*m*); δ 2.46 (*m*)
Malic acid	δ 2.68 (*dd*, J = 15.4, 3.3); δ 4.28 (*dd*, J = 9.5, 3.2)
Aspartic acid	δ 2.82 (*dd*, J = 17.0, 8.0); δ 2.95 (*dd*, J = 16.8, 4.0); δ 3.92 (*dd*, J = 8.4, 4.0)
Sucrose	δ 4.18 (*d*, J = 8.6); δ 5.41 (*d*, J = 3.8)
Glucose	δ 4.58 (*d*, J = 8.0, β-form); δ 5.19 (*d*, J = 3.8, α-form)
Fumaric acid	δ 6.52 (*s*)
Tyrosine	δ 6.85 (*d*, J = 8.5) δ 7.19 (*d*, J = 8.5)
Tryptophan	δ 7.14 (*t*, J = 7.5); δ 7.22 (*t*, J = 7.5); δ 7.29 (*s*); δ 7.48 (*d*, J = 8.0); δ 7.73 (*d*, J = 8.0)
Tryptamine	δ 7.14 (*t*, J = 7.5); δ 7.22 (*t*, J = 7.5); δ 7.28 (*s*); δ 7.48 (*d*, J = 8.0); δ 7.65 (*d*, J = 8.0)
Phenylalanine	δ 7.36 (*m*)
Formic acid	δ 8.48 (*s*)

cell lines and each cell line consists of three biological replicates. Of the identified metabolites, tryptophan, phenylalanine, tyrosine, valine, leucine, and isoleucine were significantly different ($P < 0.05$) between the groups (**Fig. 10**). It was interesting to note that the phenylalanine level was higher (about twofold) in the constitutive CrGES overexpressing cells, but lower (twofold) in the ΔplCrGES overexpressing cells, compared to the control (empty vector). The higher and lower level pattern was also observed for tyrosine, valine, and leucine. Isoleucine level in the constitutive ΔplCrGES overexpressing cell cultures was not significantly different from the control, but it was significantly higher in the constitutive CrGES overexpressing cells. For tryptophan, neither CrGES nor ΔplCrGES overexpressing cell lines were statistically different compared to the control lines but the CrGES overexpressing cells have 2.5-fold more tryptophan than that in ΔplCrGES overexpressing cells. No iridoids and TIA signals were detected in NMR, similar to the HPLC analysis. The only TIA precursor present in the samples, tryptamine was not significantly different between the groups. These results indicate that constitutive overexpression of CrGES in the plastid

and ΔplCrGES in the cytosol influenced the levels of some primary metabolites (including phenylalanine, tyrosine, and tryptophan, which derive from the shikimate pathway) while each displayed contrasting effects. There is no information on the involvement of geraniol synthase in the shikimate/phenylpropanoid pathway but there is a report by Sung et al. (2011) suggesting that the cytochrome P450 enzyme which converts geraniol to 10-oxogeranial, i.e. G8O (G10H), is not only involved in terpenoid pathway but also plays an important role in flavonoid/phenylpropanoid pathway. Further study should carry out for a better understanding of the total metabolic network.

The inducible CrGES and ΔplCrGES transgene *C. roseus* cell suspensions were also analyzed by NMR and multivariate data analysis. In the case of the inducible lines, PLS was used as supervised method and two Y-matrices were assigned, i.e. the construct groups (CrGES, ΔplCrGES, and control-empty vector) and the treatment (estradiol vs. DMSO).

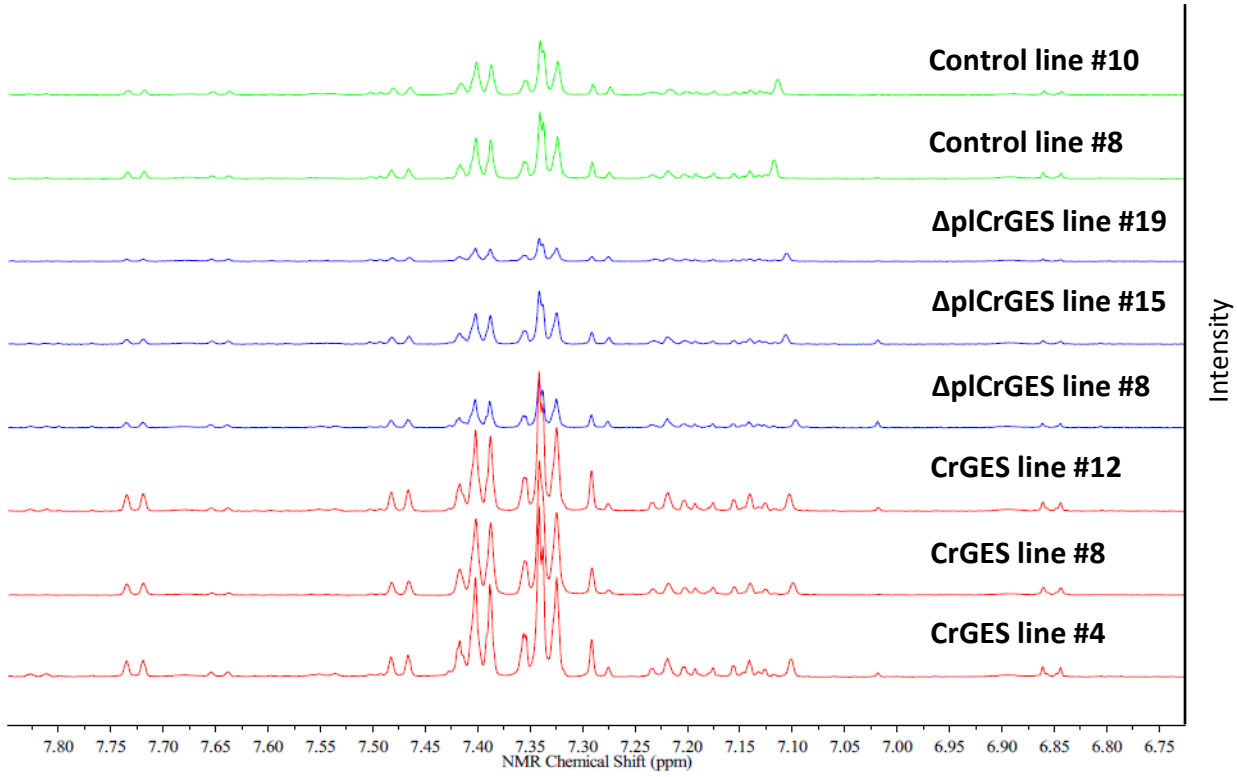

Fig. 9 Comparison of ^{1}H-NMR spectra of aromatic region of two *Catharanthus roseus* control lines (transformed with empty vector) versus different cell lines constitutively expressing CrGES and ΔplCrGES.

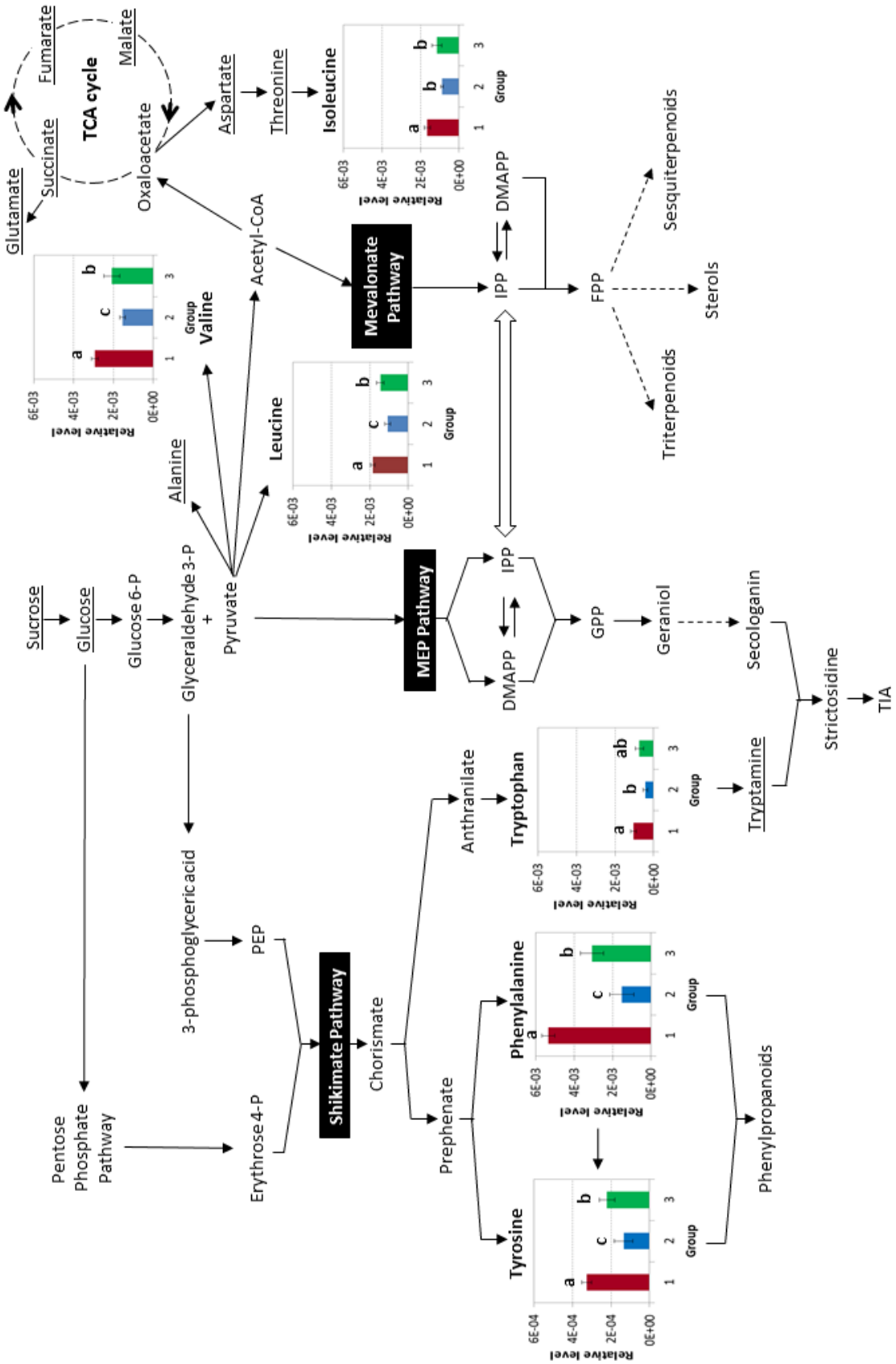

Fig. 10 Schematic representation of metabolic differences between *Catharanthus roseus* cell lines overexpressing CrGES in the plastids (1), ΔplCrGES in cytosol (2), and empty vector/control (3). Relative level of metabolites is the mean area of ^{1}H-NMR resonance peak associated to that metabolite. Each group consists of three to five different cell lines and each cell line is represented by three biological replicates. Means ± SD with different letters are significantly different ($P < 0.05$) using ANOVA followed by Duncan's Multiple Range Test (DMRT). Underlined metabolites are not significantly different in levels.

However, neither PCA nor PLS displayed separation between the lines induced with 10 µM estradiol or control (DMSO). No separation between the induced and control cell lines could be due to the observation time applied on the samples, i.e. cells were harvested 24 hours after treatment which may have been too short to develop a difference in metabolic processes between the control and induced cell lines.

Conclusion

In this study, we describe the development of *C. roseus* cell lines overexpressing geraniol synthase in the plastid (CrGES) or the cytosol (ΔplCrGES). The study confirmed the expression of CrGES and ΔplCrGES in both subcellular compartments. However, geraniol was not detected in the transformed cells, or present below the detection limit. Further analyses are needed to reveal if the GES product is formed and subsequently derivatized to glycosylated geraniol products. No accumulation of TIA or iridoid pathway precursors was detected in the *C. roseus* cells of the line MP183L after overexpressing geraniol synthase, whereas jasmonate acid elicitation did not cause clear differences in TIA production between overexpression and control cultures. NMR-based metabolomics combined with multivariate data analysis revealed some primary metabolites associated to the separation of the constitutive CrGES, ΔplCrGES *C. roseus* cells and controls in PLS-DA/OPLS-DA analysis. In contrast to a higher level of several metabolites of which some are associated to shikimate pathway in the constitutive CrGES overexpressing *C. roseus* cells, a lower level of these metabolites was detected in the ΔplCrGES overexpressing cultures compared to the control, thus suggesting different metabolic effects related to the subcellular compartmentation of geraniol synthase.

Acknowledgements

The authors thank Mr. Ward de Winter for preparing the cell culture media and Ms. Gerda Lamers for assistance with the microscopy observations. The authors also thank the Ministry of Education Malaysia and University of Malaya (Malaysia) for the financial support of Mohd Zuwairi Saiman. This research was funded by the IBOS-ACTS program as coordinated by NWO.

References

Canel C, Lopes-Cardoso MI, Whitmer S, van der Fits L, Pasquali G, van der Heijden R, Hoge JHC, Verpoorte R (1998) Effects of overexpression of strictosidine synthase and tryptophan decarboxylase on alkaloid production by cell cultures of *Catharanthus roseus*. Planta 205: 414–419

Contin A, van der Heijden R, Lefeber AW, Verpoorte R (1998) The iridoid glucoside secologanin is derived from the novel triose phosphate/pyruvate pathway in a *Catharanthus roseus* cell culture. FEBS Lett 434: 413–416

Dong L, Miettinen K, Goedbloed M, Verstappen FW, Voster A, Jongsma MA, Memelink J, van der Krol S, Bouwmeester HJ (2013) Characterization of two geraniol synthases from *Valeriana officinalis* and *Lippia dulcis*: similar activity but difference in subcellular localization. Metab Eng 20: 198–211

Fischer MJ, Meyer S, Claudel P, Bergdoll M, Karst F (2011) Metabolic engineering of monoterpene synthesis in yeast. Biotechnol Bioeng 108: 1883–1892

Ishige F, Takaichi M, Foster R, Chua NH, Oeda K (1999) A G-box motif (GCCACGTGCC) tetramer confers high-level constitutive expression in dicot and monocot plants. Plant J 18: 443–448

Jaggi M, Kumar S, Sinha AK (2011) Overexpression of an apoplastic peroxidase gene *CrPrx* in transgenic hairy root lines of *Catharanthus roseus*. Appl Microbiol Biotechnol 90: 1005–1016

Linsmaier EM, Skoog F (1965) Organic growth factor requirements of tobacco tissue cultures. Physiol Plant 18: 100–127

Liu DH, Ren WW, Cui LJ, Zhang LD, Sun XF, Tang KX (2011) Enhanced accumulation of catharanthine and vindoline in *Catharanthus roseus* hairy roots by overexpression of transcriptional factor ORCA2. Afr J Biotechnol 10: 3260–3268

Magnotta M, Murata J, Chen J, De Luca V (2007) Expression of deacetylvindoline-4-*O*-acetyltransferase in *Catharanthus roseus* hairy roots. Phytochemistry 68: 1922–1931

Martin D, Piulachs MD, Cunillera N, Ferrer A, Bellés X (2007) Mitochondrial targeting of farnesyl diphosphate synthase is a widespread phenomenon in eukaryotes. Biochim Biophys Acta 1773: 419–26

Memelink J, Swords KMM, Staehelin LA, Hoge JHC (1994) Southern, Northern and Western blot analysis. In: Gelvin SB, Schilperoot RA (eds.) Plant Molecular Biology Manual. Kluwer Academic Publishers, Dordrecht, pp. 273–295

Moreno PRH, van der Heijden R, Verpoorte R (1995) Cell and tissue cultures of *Catharanthus roseus*: a literature survey. Plant Cell Tiss Organ Cult 42: 1–25

Nelson BK, Cai X, Nebenführ A (2007) A multicolored set of in vivo organelle markers for co-localization studies in *Arabidopsis* and other plants. Plant J 51: 1126–1136

Niwa Y (2003) A synthetic green fluorescent protein gene for plant biotechnology. Plant Biotechnol 20: 1–11

Pan Q, Wang Q, Yuan F, Xing S, Zhao J, Choi YH, Verpoorte R, Tian Y, Wang G, Tang K (2012) Overexpression of ORCA3 and G10H in *Catharanthus roseus* plants regulated alkaloid

biosynthesis and metabolism revealed by NMR-metabolomics. PLoS ONE 7(8):e43038. doi:10.1371/journal.pone.0043038

Peebles CA, Hughes EH, Shanks JV, San KY (2009) Transcriptional response of the terpenoid indole alkaloid pathway to the overexpression of ORCA3 along with jasmonic acid elicitation of *Catharanthus roseus* hairy roots over time. Metab Eng 11: 76–86

Peebles CAM, Sander GW, Hughes EH, Peacock R, Shanks JV, San KY (2010) The expression of 1-deoxy-D-xylulose synthase and geraniol 10-hydroxylase or anthranilate synthase increases terpenoid indole alkaloid accumulation in *Catharanthus roseus* hairy roots. Metab Eng 13: 234–40

Pomahačová BDJ, Dusková J, Yazaki K, Roytrakul S, Verpoorte R (2009) Improved accumulation of ajmalicine and tetrahydroalstonine in *Catharanthus* cells expressing an ABC transporter. J Plant Physiol 166: 1405–1412.

Rohmer M (1999) The discovery of a mevalonate-independent pathway for isoprenoid biosynthesis in bacteria, algae and higher plants. Nat Prod Rep 16:565–574

Saiman MZ, Mustafa NR, Pomahačová B, Verberne M, Verpoorte R, Choi YH, Schulte AE (2014) Analysis of metabolites in the terpenoid pathway of *Catharanthus roseus* cell suspensions. Plant Cell Tiss Organ Cult 117: 225–239

Sapir-Mir M, Mett A, Belausov E, Tal-Meshulam S, Frydman A, Gidoni D, Eyal Y (2008) Peroxisomal localization of Arabidopsis isopentenyl diphosphate isomerases suggests that part of the plant isoprenoid mevalonic acid pathway is compartmentalized to peroxisomes. Plant Physiol 148: 1219–1228

Simkin AJ, Guirimand G, Papon N, Courdavault V, Thabet I, Ginis O, Bouzid S, Giglioli-Guivarc'h N, Clastre M (2011) Peroxisomal localisation of the final steps of the mevalonic acid pathway in planta. Planta 234: 903–914

Simkin AJ, Miettinen K, Claudel P, Burlat V, Guirimand G, Courdavault V, Papon N, Meyer S, Godet S, St-Pierre B, Giglioli-Guivarc'h N, Fischer MJ, Memelink J, Clastre M (2013) Characterization of the plastidial geraniol synthase from Madagascar periwinkle which initiates the monoterpenoid branch of the alkaloid pathway in internal phloem associated parenchyma. Phytochemistry 85: 36–43

Sung PH, Fong-Chin Huang FC, Do YY, Pung-Ling Huang PL (2011) Functional expression of geraniol 10-hydroxylase reveals its dual function in the biosynthesis of terpenoid and phenylpropanoid. J Agric Food Chem 59: 4637–4643

Thabet I, Guirimand G, Courdavault V, Papon N, Godet S, Dutilleu C, Bouzid S, Giglioli-Guivarc'h N, Clastre M, Simkin AJ (2011) The subcellular localization of periwinkle farnesyl diphosphate synthase provides insight into the role of peroxisome in isoprenoid biosynthesis. J Plant Physiol 168: 2110–2116

Töpfer R, Matzeit V, Gronenborn B, Schell J, Steinbiss HH (1987) A set of plant expression vectors for transcriptional and translational fusions. Nucleic Acids Res 15: 5890

van der Fits L, Memelink J (1997) Comparison of the activities of CaMV 35S and FMV 34S promoter derivatives in *Catharanthus roseus* cells transiently and stably transformed by particle bombardment. Plant Mol Biol 33: 943–946

van der Fits L, Memelink J (2000) ORCA3, a jasmonate-responsive transcriptional regulator of plant primary and secondary metabolism. Science 289: 295–297

van der Heijden R, Verpoorte R, Ten Hoopen HJG (1989) Cell and tissue cultures of *Catharanthus roseus* (L.) G. Don: a literature survey. Plant Cell Tiss Organ Cult 18: 231–280

van der Heijden R, Jacobs DI, Snoeijer W, Hallard D, Verpoorte R (2004) The *Catharanthus* alkaloids: pharmacognosy and biotechnology. Curr Med Chem 11: 607–628

Verpoorte R, Contin A, Memelink J (2002) Biotechnology for the production of plant secondary metabolites. Phytochem Rev 1: 13–25

Verpoorte R, van der Heijden R, Memelink J (2000) Engineering the plant cell factory for the secondary metabolite production. Transgenic Res 9: 323-343

Wang CT, Liu H, Gao XS, Zhang HX (2010) Overexpression of G10H and ORCA3 in the hairy roots of *Catharanthus roseus* improves catharanthine production. Plant Cell Rep 29: 887–894

Westerhuis JA, van Velzen EJJ, Hoefsloot HCJ, Smilde AK (2010) Multivariate paired data analysis: multilevel PLSDA versus OPLSDA. Metabolomics 6: 119–128

Whitmer S, van der Heijden R, Verpoorte R (2002) Effect of precursor feeding on alkaloid accumulation by a strictosidine synthase over-expressing transgenic cell line S1 of *Catharanthus roseus*. Plant Cell Tissue Organ Cult 69:85–93

Wu S, Schalk M, Clark A, Miles RB, Coates R, Chappell J (2006) Redirection of cytosolic or plastidic isoprenoid precursors elevates terpene production in plants. Nat Biotechnol 24: 1441– 1447

Zhao J, Verpoorte R (2007) Manipulating indole alkaloid production by *Catharanthus roseus* cell cultures in bioreactors: from biochemical processing to metabolic engineering. Phytochem Rev 6: 435–457

Zuo J, Niu QW, Chua NH (2000) An estrogen receptor-based transactivator XVE mediates highly inducible gene expression in transgenic plants. Plant J 24: 265–273

Supplement 1 The full-length cDNA of *Catharanthus roseus* geraniol synthase (CrGES) localized in the plastid (Genbank ID: JN882024). Its plastidial leader peptide was predicted to be at least 43 amino acids in length (Simkin et al. 2013). The underlined sequence indicates the first 156 bp (52 amino acids; until the first ATG-methionine following the leader) which were deleted to make the truncated version of ΔplCrGES in this study.

ATGGCAGCCACAATTAGTAACCTTTCTTTCTTAGCAAAATCTAGGGCACTTTCAAGGCCTTCTTCTTCTTCACTT
TCATGGCTAGAAAGGCCTAAAACTTCATCGACTATTTGCATGTCTATGCCATCATCTTCATCATCATCATCATCT
TCATCCATGTCTCTGCCTTTGGCAACTCCATTGATCAAAGACAATGAATCTCTCATCAAGTTCTTGCGCCAACCC
CTGGTGCTTCCTCATGAGGTTGATGACAGCACAAAAAGGAGGGAATTGTTGGAAAGAACAAGAAAAGAACTAGAA
TTAAATGCAGAAAAACCATTGGAGGCCTTGAAGATGATAGATATAATTCAAAGATTGGGATTATCATATCATTTT
GAAGATGATATTAATTCAATTCTCACAGGATTTTCAAATATTAGCAGCCAAACTCATGAAGATCTCCTCACTGCT
TCACTTTGTTTTCGATTGCTTCGACACAATGGGCATAAGATCAATCCTGATATATTCCAAAAATTCATGGACAAC
AATGGAAAGTTTAAAGATTCATTAAAGGATGACACATTAGGCATGTTAAGCTTATATGAAGCTTCATATTTGGGA
GCCAATGGAGAAGAAATATTGATGGAAGCCCAAGAATTCACCAAAACTCACCTGAAAAACTCATTGCCAGCCATG
GCACCATCTCTTTCTAAGAAGGTTTCTCAAGCTTTAGAGCAACCAAGACATAGAAGAATGTTGAGGTTAGAAGCT
AGAAGATTTATTGAAGAATATGGTGCTGAAAATGACCATAATCCAGACCTTCTTGAGCTTGCAAAATTGGATTAT
AACAAAGTCCAATCTCTACACCAAATGGAATTGTCTGAGATAACAAGGTGGTGGAAACAATTAGGGCTTGTGGAT
AAACTCACCTTTGCTCGAGATCGACCCCTTGAATGCTTTCTTTGGACAGTGGGATTATTACCAGAGCCTAAGTAT
TCAGGTTGCAGAATTGAGCTTGCAAAAACCATAGCCATTTTGCTTGTCATTGATGATATCTTTGATACTCATGGT
ACCCTAGATGAGCTTCTTCTATTCACTAATGCCATTAAAAGATGGGATCTTGAGGCCATGGAAGATTTACCAGAA
TATATGAGAATTTGTTACATGGCATTGTACAATACTACTAATGAAATTTGCTATAAAGTTCTTAAGGAAAATGGT
TGGAGTGTTCTTCCTTACCTAAAGGCAACGTGGATTGATATGATTGAAGGATTCATGGTTGAAGCAGAATGGTTC
AATTCTGATTATGTACCAAACATGGAAGAATATGTAGAAAATGGAGTTAGAACAGCAGGATCATATATGGCCTTA
GTCCATTTGTTCTTTCTAATAGGGCAAGGTGTCACTGAAGATAATGTGAAATTACTGATTAAACCCTATCCAAAG
CTCTTTTCCTCCTCAGGAAGAATCCTTCGCCTTTGGGATGATTTGGGAACTGCAAAGGAGGAACAAGAAAGAGGA
GACTTGGCATCAAGCATACAATTGTTTATGAGAGAGAAAGAGATAAAATCAGAAGAAGAAGGAAGGAAAGGAATA
TTGGAAATTATAGAGAATTTATGGAAAGAATTGAATGGAGAATTAGTTTATAGAGAAGAAATGCCTCTTGCAATA
ATCAAGACAGCATTCAACATGGCAAGAGCTTCCCAAGTTGTGTATCAACATGAAGAAGACACCTATTTTTCAAGT
GTAGATAATTATGTAAAAGCTTTGTTTTTTACACCTTGTTTTTAA

Supplement 2 The primer sequences used for designing full-length cDNA of *Catharanthus roseus* geraniol synthase (CrGES) or a truncated version without its plastidial leader peptide (ΔplCrGES). Construct no. 1 and 2 are the inserts for constitutive and inducible expression. Construct no. 3 and 4 are the inserts for transient expression.

No	Constructs	Primer sequences	
		Forward	Reverse
1.	*SalI*-CrGES-*XbaI*	5'-GTCGACAAAATGGCAGCCACAATTAGTAACC-3'	5'-TCTAGATTAAAAACAAGGTGTAAAAAACAAAGC-3'
2.	*SalI*-ΔplCrGES-*XbaI*	5'-GTCGACAAAATGTCTCTGCCTTTGGCAACT-3'	5'-TCTAGATTAAAAACAAGGTGTAAAAAACAAAGC-3'
3.	*SalI*-CrGES-*SalI*	5'-GTCGACAAAATGGCAGCCACAATTAGTAACC-3'	5'-GTCGACAAAACAAGGTGTAAAAAACAAAGC-3'
4.	*SalI*-ΔplCrGES-*SalI*	5'-GTCGACAAAATGTCTCTGCCTTTGGCAACT-3'	5'-GTCGACAAAACAAGGTGTAAAAAACAAAGC-3'

Supplement 3 The PCR products cut with restriction enzymes *SalI* and *XbaI* examined by gel electrophoresis. 1) full-length fragment of *Catharanthus roseus* geraniol synthase (CrGES; about 1.8 kb). 2) fragment encoding truncated CrGES without plastidial leader peptide (ΔplCrGES; about 1.6 kb).

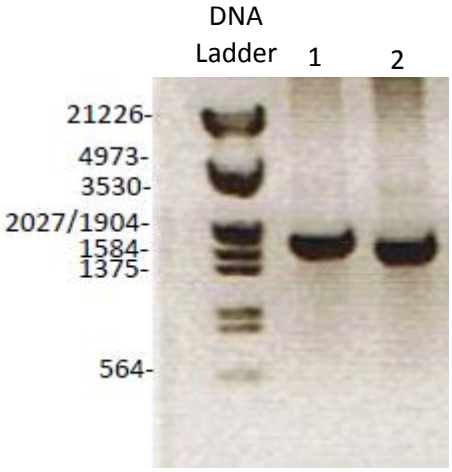

Supplement 4 Constructs of pTH2-Δ*EcoRI*::CrGES-GFP (A) and pTH2-Δ*EcoRI*::Δpl CrGES-GFP (B) excised with *BglII/PstI* give expected sizes of DNA bands as represented in the construct scheme (C). Correct construct (√), empty vector (0), and reverse insert (x).

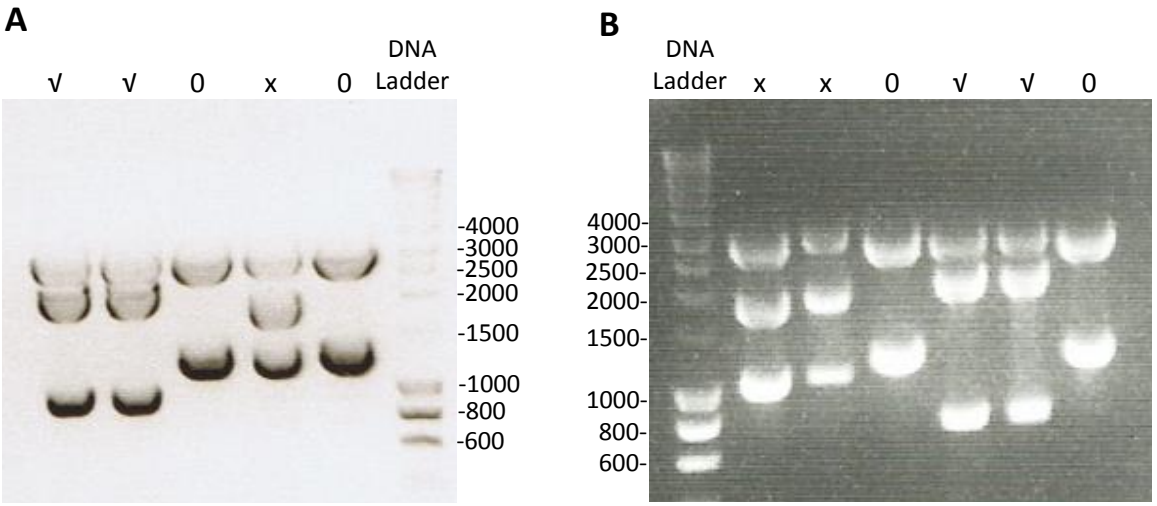

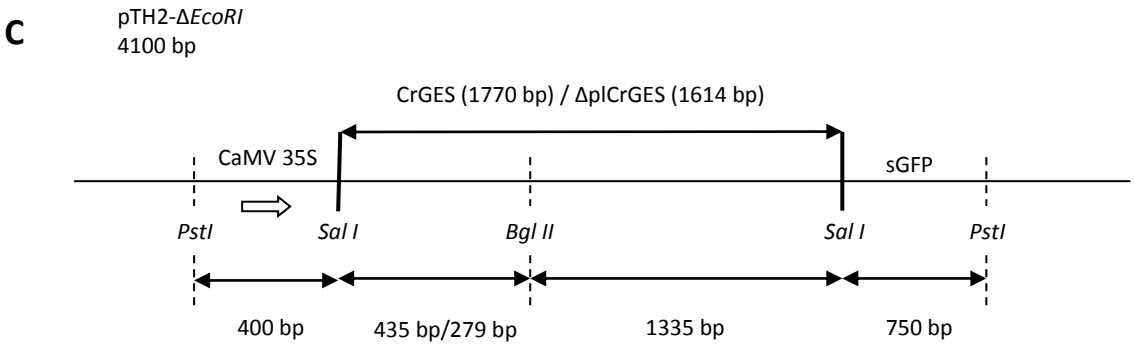

Supplement 5 Constructs of pRT101::CrGES (A) excised with *BglII/PstI* (1 – 5) and pRT101::ΔplCrGES (B) excised with *BglII/PstI* (1, 2) and *PstI* (3) give expected sizes of DNA bands as represented in the construct scheme (C).

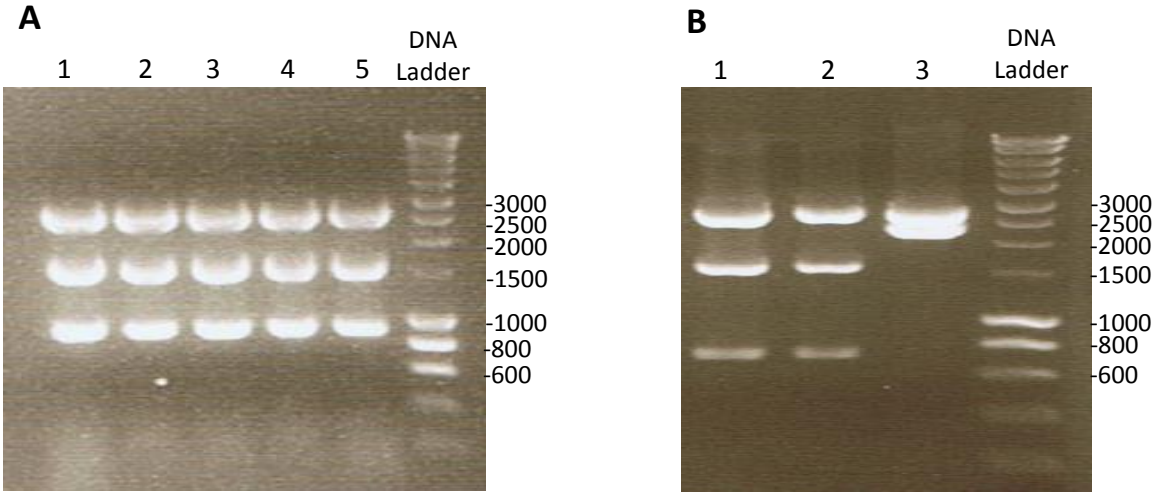

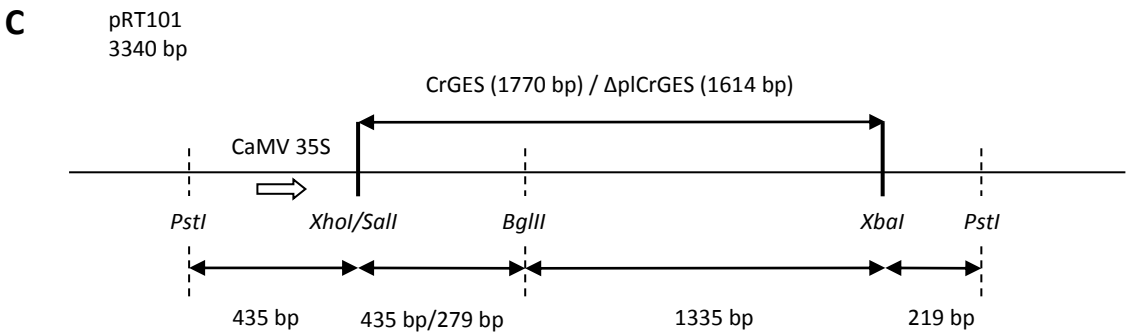

Supplement 6 Constructs of pER8::CrGES (A) and pER8::ΔplCrGES (B) excised with *BglII* give expected sizes of DNA bands as represented in the construct scheme (C).

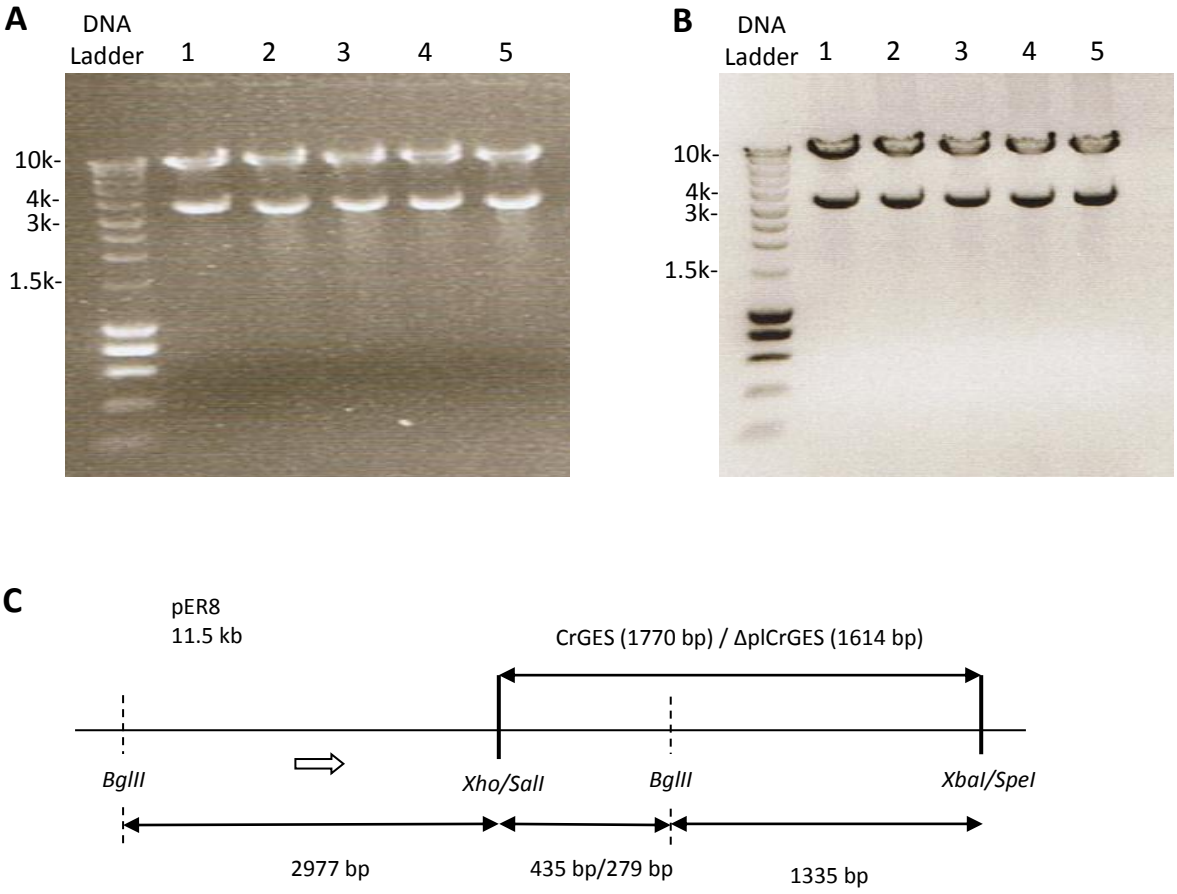

Supplement 7 A study on transformation efficiency between cell-line MP183L (A) and CRPP (B) bombarded with 35S-GUS plasmid. Blue spots after histochemical staining with X-Gluc are caused by GUS activity.